Australian Government
Geoscience Australia

INTEGRATED EXPLORATION IN A CHANGING WORLD
ASEG-PESA
SYDNEY 2004

Airborne Gravity 2004

Abstracts from the ASEG-PESA Airborne Gravity 2004 Workshop

Edited by Richard Lane

Record
2004/18

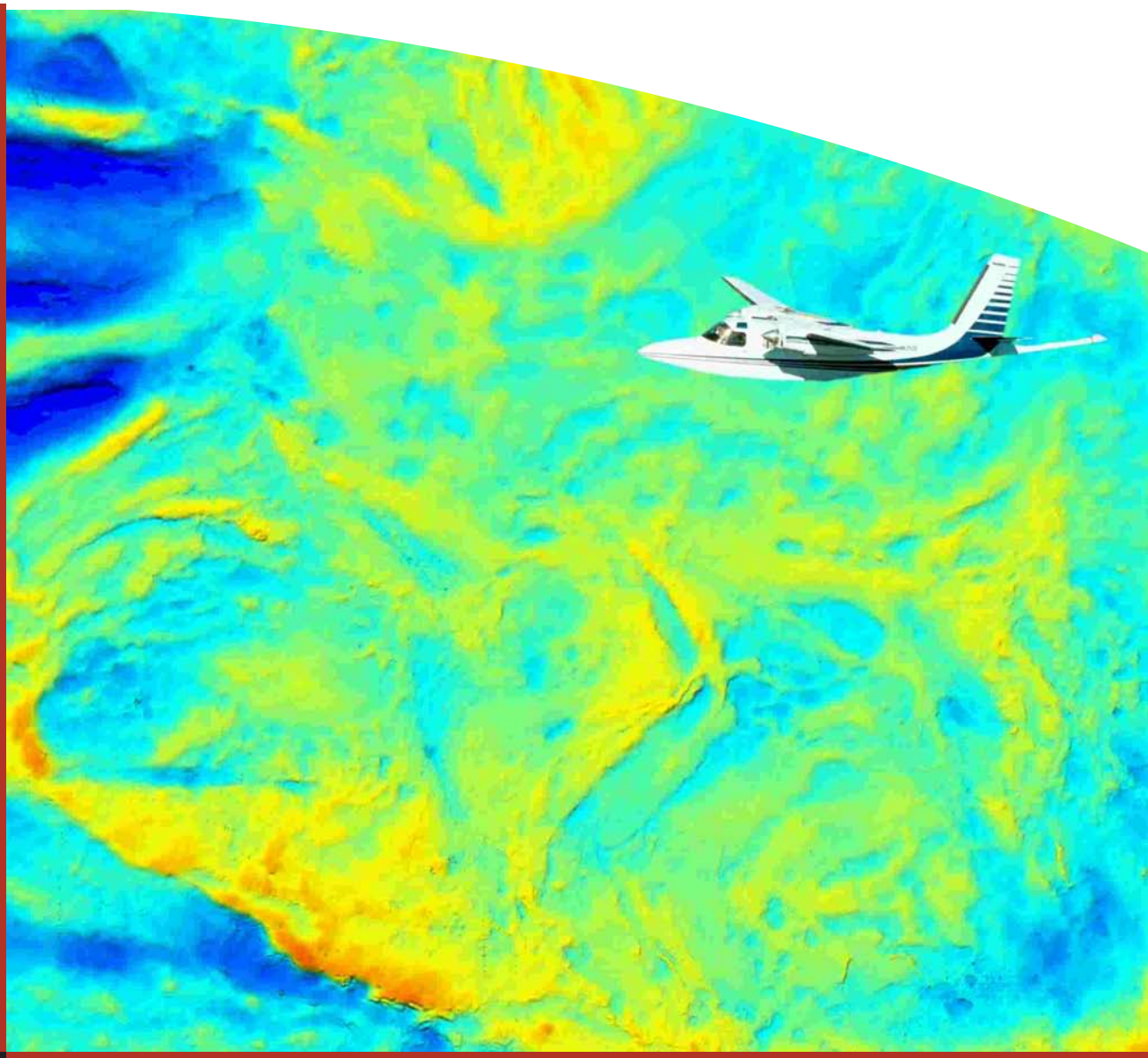

Geoscience Australia Record 2004/18

Airborne Gravity 2004

Abstracts from the ASEG-PESA Airborne Gravity 2004 Workshop

Edited by Richard Lane

Department of Industry, Tourism & Resources

Minister for Industry, Tourism & Resources: The Hon. Ian Macfarlane, MP
Parliamentary Secretary: The Hon. Warren Entsch, MP
Secretary: Mark Paterson

Geoscience Australia

Chief Executive Officer: Neil Williams

ISSN: 1448-2177
ISBN: 1 920871 13 6

GeoCat no. 61129

Bibliographic Reference:

a) For the entire publication

Lane, R.J.L., editor, 2004, Airborne Gravity 2004 – Abstracts from the ASEG-PESA Airborne Gravity 2004 Workshop: *Geoscience Australia Record* 2004/18.

b) For an individual paper

van Kann, F., 2004, Requirements and general principles of airborne gravity gradiometers for mineral exploration, in R.J.L. Lane, editor, Airborne Gravity 2004 - Abstracts from the ASEG-PESA Airborne Gravity 2004 Workshop: *Geoscience Australia Record* 2004/18, 1-5.

Contents

"Airborne Gravity 2004 Workshop" Record

Richard Lane
Geoscience Australia
richard.lane@ga.gov.au

Mark Dransfield
BHP Billiton
Mark.H.Dransfield@bhpbilliton.com

David Robson
NSW Department of Primary Industry – Minerals
david.robson@minerals.nsw.gov.au

Robert Smith
Greenfields Geophysics
greengeo@bigpond.net.au

Greg Walker
BHP Billiton
Greg.B.Walker@BHPBilliton.com

Preface

The "Airborne Gravity 2004 Workshop" was held in Sydney on August 15, in conjunction with ASEG-PESA Sydney 2004 (the ASEG's 17th Geophysical Conference and Exhibition). The aims of the workshop were to provide participants with a review of the current state of the art in airborne gravity instrumentation, to present case histories of the use of these methods in minerals and petroleum applications, and to distribute sample data sets. "Airborne gravity" is used in this context to include both airborne gravimeter and airborne gravity gradiometer methods.

The program was split into 2 sessions. The morning session provided a review of the systems, with presentations covering a number of systems currently in operation as well as some that are still under development. The focus shifted in the afternoon session to case histories, with examples from surveys spanning the globe; from Antarctica to the tropics of Papua New Guinea, from Africa through Australia to Canada.

To capture the essence of the day and to promote the ongoing development of airborne geophysical methods, speakers were invited to submit papers for inclusion in a workshop volume. The papers were reviewed prior to publication in this Geoscience Australia Record. Participants received a copy at the workshop, and additional copies of the Record are available on an ongoing basis from Geoscience Australia (www.ga.gov.au).

Units

Physical quantities should be expressed in SI units. The Bureau International des Poids et Mesures (BIPM) is the custodian of this system. To quote from their website (www.bipm.fr): "Its mandate is to provide the basis for a single, coherent system of measurements throughout the world, traceable to the International System of Units (SI)".

The SI unit for acceleration is "metre per second squared" (m/s^2). The signals encountered in gravity surveys for exploration are small, and the prefix "micro" is commonly used (micrometre per second squared, $\mu m/s^2$). The gal (or Gal), equal to 1 cm/s^2, is a derived unit for acceleration in the CGS system of units. A prefix of "milli" is commonly used (milligal, mGal). In rare cases in the literature, a "gravity unit" (gu) may be encountered. In this publication, the $\mu m/s^2$ has been the preferred unit for gravity measurements, but mGal has been accepted.

1 $\mu m/s^2 = 10^{-6}$ m/s^2
1 mGal = 10 $\mu m/s^2$
1 gu = 1 $\mu m/s^2$

The gravity gradient is a gradient of acceleration and so the appropriate units are acceleration units divided by distance units. Thus, "per second squared" (s^{-2}) is appropriate in the SI system. Typical gravity gradients measured in exploration are extremely small, and the prefix "nano" is appropriate in most circumstances (per

nanosecond squared, ns^{-2}). The eotvos unit (Eo), although not recognised in either the SI or CGS systems, is used almost universally in geophysics as the unit for gravity gradient measurements. It is equal to 1 ns^{-2}. In this publication, the ns^{-2} and Eo have both been accepted as units for gravity gradient measurements.

$1\ ns^{-2} = 10^{-9}\ s^{-2}$
$1\ Eo = 1\ ns^{-2}$

Acknowledgments

The Airborne Gravity 2004 Workshop Organising Committee would like to acknowledge the support of the ASEG-PESA 2004 Conference Organizing Committee and the Conference Secretariat. Support from Geoscience Australia, BHP Billiton and the NSW Department of Primary Industries - Mineral Resources helped to make the workshop a success. The diligence of Mario Bacchin, Katharine Hagan, Angie Jaensch, Jim Mason, Peter Milligan, Ian Hone and Roger Clifton enabled this Record to be produced in time for the Workshop, despite a tight deadline. Finally, a vote of thanks goes to the speakers who committed their time and energy to deliver presentations on the day and to compose this permanent record of the event.

Integrating ground and airborne data into regional gravity compilations

Richard Lane
Geoscience Australia
richard.lane@ga.gov.au

Abstract

A procedure for taking vertical gravity data from an airborne gravity (AG) or airborne gravity gradiometry (AGG) survey and combining it with vertical gravity data from ground measurements to produce a regional compilation is described. The method is illustrated using examples of AG data from West Arnhem Land (Northern Territory, Australia) and AGG data from Broken Hill (New South Wales, Australia). Despite significant differences in the acquisition and processing methods used for AG and AGG data, the integration procedure is the same for both. The procedure takes into account that the airborne and ground datasets are measured on different drape surfaces, that long wavelengths are not properly recovered in the airborne datasets, and that noise produces inconsistencies where surveys overlap in horizontal position.

Before combining the two datasets, the input ground and airborne datasets are continued upwards or downwards to the chosen output drape surface using a drape-to-drape continuation procedure. Gaps in the long wavelength information content of the airborne data are filled with long wavelength information from the ground data using a technique termed “crossover” filtering.

A smooth combined output data surface is obtained by jointly inverting the datasets using an equivalent source technique configured with a regular grid of sources. The spatial smoothness of the mass properties for the sources, and hence the smoothness of the fitted potential field surface, is controlled to produce data misfits consistent with the estimates of uncertainty supplied for each data point.

This procedure requires not just the data values and horizontal locations of the observations, but information concerning the vertical position or elevation surface for each dataset, the range of wavelengths present in each dataset and estimates of the uncertainty in the data values. This information is not always readily available, and much effort in the examples was spent on these issues.

The integrated product does not entirely replace the input ground and airborne datasets for interpretation purposes. However, the integrated product adds value because it has a different spectral mix compared with either of the inputs. In the examples that are presented, accurate long wavelength information from the ground data is merged with accurate mid-wavelength information from the airborne data. Additionally, information is carried through to the output from small prospect areas which have detailed and accurate ground data. The combination method described here differs in this respect from the crossover filtering method of combining data which simply replaces the ground data with airborne data within the boundaries of the airborne survey.

Introduction

The present ground gravity coverage of Australia is accurate at the longest wavelengths that are of interest for petroleum and minerals applications (i.e., from tens to hundreds of kilometres). Stations are no more than 11 km apart and observations are tied to the Australian Fundamental Gravity Network. Ground and airborne data acquisition methods are being used by explorers and governments to provide greater detail at short to intermediate wavelengths in specific areas of greater interest. When deciding whether to use ground or airborne methods for this purpose, there is a trade-off between the greater accuracy of ground data and the benefits of decreased acquisition time for large survey areas and avoiding the need for direct land access that are associated with the use of airborne methods.

There are two classes of airborne systems that can provide vertical gravity data; airborne gravity (AG) and airborne gravity gradiometry (AGG) systems.

Airborne gravity (AG) systems measure vertical acceleration using a single sensor. Independent measurement of the motion of the aircraft via GPS navigation information allows inertial acceleration to be calculated and subtracted from the total acceleration, leaving the component of acceleration due to gravity. The uncertainty in GPS produces errors in the inertial acceleration calculation that rise in amplitude as wavelength decreases (see Figure 2.2 of Bruton, 2000). This noise is suppressed by low-pass filtering thus

limiting resolution at short wavelengths. The long wavelength performance is limited by the linearity and rate of drift of the accelerometer output (again, see Figure 2.2 of Bruton, 2000).

The airborne gravity gradiometer (AGG) systems that are presently being operated use complements of four acceleration sensors mounted on rotating disks (Lee, 2001). The inertial acceleration of the disk is common to all sensors, and combinations of the sensor outputs can be used to estimate gradients of the acceleration due to gravity in the plane of the disk. The AGG systems measure two or more components of the gravity gradient tensor depending on the number of disks present and their orientation. The gradients measured at different locations can be transformed to vertical gravity. Residual inertial acceleration effects induced by turbulence limit the performance at short wavelengths. Long wavelength performance is limited principally by the size of the survey and the truncation errors obtained by integration of gradient signals over a finite area to derive vertical gravity.

For an integrated product that combines ground and airborne gravity data to be useful for interpretation purposes, it should cover a larger area than the airborne survey, and thus provide context for the airborne survey data. The integration procedure should not simply involve replacing the ground data with the airborne data within the survey area, but allow detailed and accurate ground data to enhance the airborne data where such data are present within the bounds of the survey area. Since airborne methods are unable to completely capture the longer wavelengths, the final product should include the long wavelength control provided by ground gravity data. A method to integrate ground and airborne gravity data that satisfies these conditions is described in the following section. This method is then demonstrated using field examples of AG and AGG data in combination with ground gravity data.

Method

The ideal method to combine vertical gravity data from ground and airborne observations and output a grid of vertical gravity on a specified drape surface would need to address a number of specific characteristics of the problem. The ground and airborne data relate to locations on different irregular drape surfaces. The chosen output drape surface may or may not correspond to either of these surfaces. Both datasets contain noise which means there will be inconsistencies between the values where the datasets overlap. This noise will introduce instability into any prediction of vertical gravity closer to the source than the original observation (i.e., during downward continuation). The airborne data have been filtered, which modifies the response from the theoretical broadband response and produces correlation between the data errors. The datasets may also be very large, which will introduce computation difficulties.

Schematic sections in Figure 1 illustrate the geometrical aspects of an idealized equivalent source procedure for combining the two datasets. The ground and airborne data would be jointly inverted using a set of equivalent source elements as the model (Figure 1a). The forward modeling algorithm used to generate predicted data for each of the source elements would account for the filtering of airborne observations. Constraints on the spatial variability of the mass properties of the sources would be used to produce a smooth fit to the observations and hence resolve inconsistencies between the datasets. The data misfit calculation would incorporate supplied estimates of the noise for each observation, and allow for any specified correlation between these errors. Having solved the inverse problem, the vertical gravity response on the output drape surface could be predicted by forward modeling (Figure 1b). Either a wideband or filtered response could be generated as required.

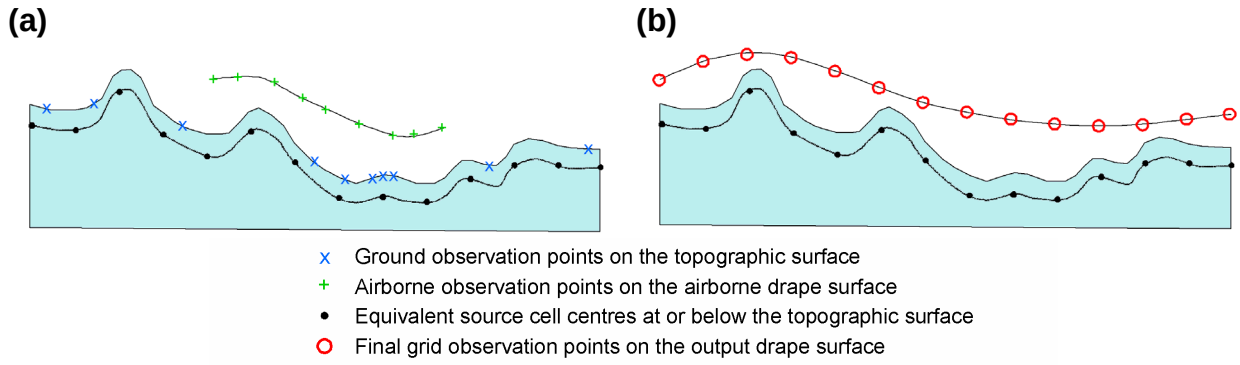

Figure 1. Schematic sections showing an idealised equivalent source procedure. (a) Invert ground and airborne observations for an equivalent source distribution immediately below the ground surface. (b) Forward model the equivalent source distribution at regular locations on the output drape surface. The output drape surface may or may not coincide with either of the topographic or airborne drape surfaces.

Unfortunately, the method described above has not been implemented in any of the readily available geophysical software programs. An alternate procedure was formulated making use of available tools. The geometrical aspects of this procedure are illustrated in Figure 2.

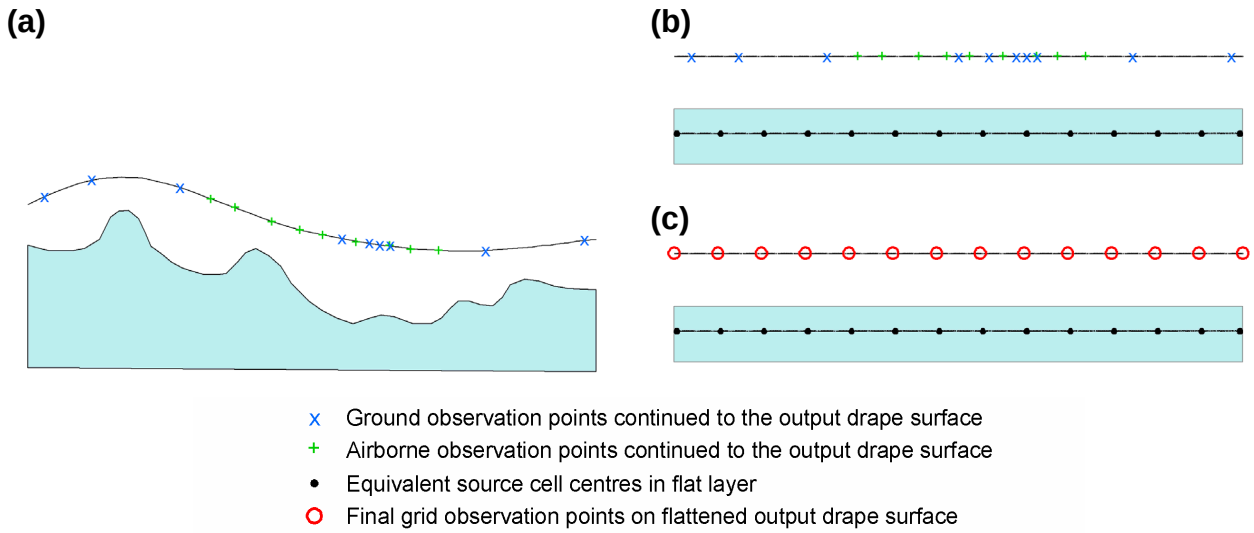

Figure 2. Schematic sections showing the actual method used in the examples. (a) Continue ground and airborne observations as shown in Figure 1(a) onto a smooth output drape surface. Then apply "crossover" filtering to the airborne data (not shown). (b) Assume the observations are now on a flat surface and invert for an equivalent source distribution on a horizontal surface below the flattened output drape surface. (c) Forward model the equivalent source distribution at regular locations on the flattened output drape surface.

Both datasets are first continued onto the output drape surface (Figure 2a) using a drape-to-drape method (Cordell and Grauch, 1985). For this procedure, the datasets are required to be in gridded format. The airborne datasets used in this study were supplied in gridded form, so no further pre-processing of them was required. The ground data were supplied in point located form, so these data were gridded using a minimum curvature method. It is arguable whether to upward continue the ground data to the level of the airborne drape surface or to downward continue the airborne data to the ground surface. The appearance of the short wavelength information in the combined product will be influenced by this choice of output drape surface. Although the short wavelength information will be more prominent in the output if the output surface is close to the ground surface, the actual signal to noise ratio in the short wavelengths will be independent of the choice of elevation surface. Due to the presence of noise, low-pass filtering of the airborne data would be required if the airborne data were required to be downward continued. This would essentially defeat the true purpose of downward continuation. Thus, the output drape surface was always chosen to be at or above the airborne drape surface.

The poorly-resolved longer wavelengths in the airborne data were replaced with more accurate information from ground data using a grid-based "crossover" filtering technique (Hensley, 2003c). For this procedure, a grid-based high-pass filter was first applied to the airborne data, and then the complementary low-pass filter was applied to the ground data. The filtered products were added together to produce a modified airborne dataset which can now be integrated with ground data.

The pre-processing of the data up until this point is designed to minimize the errors associated with simplifying conditions used when jointly fitting a smooth surface to both datasets. The two datasets are assumed to have full spectral content when in actual fact the airborne data have been low-pass filtered, and the datasets are assumed to be observations on a level surface when the observations have actually been continued to the output drape surface that may not be level.

A 3D gravity inversion program described by Li and Oldenburg (1998) was used for the equivalent source inversion. To simplify the geometry of the density layer and reduce the computational requirement, a single layer of close-packed rectangular prisms with square horizontal cross section and vertical extent 10 times their horizontal extent was used. The purpose of the equivalent source inversion was to produce a smooth fit to the two datasets that is consistent with expectations from the supplied noise estimates rather than to faithfully model the actual geometry of the observations. Provided that the output drape surface was sufficiently smooth, the errors introduced by using a flattened approximation of the true geometry as illustrated in Figure 2(b) and (c) would be small. The depth extent of the prisms has an effect on the density values produced by the inversion, but has no real impact on the fit obtained. Prisms with horizontal extent equal to the cell size in the desired combined regional grid were used, with a depth to top equal to the

horizontal extent. These parameters were chosen so that the structure of the model would not contribute to the regularization of the inversion problem, and hence would not impede the desired smooth fit from being obtained. Explicit regularization in the form of lateral “smoothness” and “smallness” constraints on the mass properties of the source elements was used by the inversion program to produce a chi-squared data misfit appropriate to the uncertainty values of the supplied data. To facilitate application of a “smallness” constraint, a first order trend surface was removed from the data prior to inversion. Unfortunately, the basic processing tools available did not allow the missing or aliased short wavelength information of the datasets to be taken into account. These tools also assumed that the errors in the data values were Gaussian and uncorrelated. The latter assumption is false for the airborne data given that spatial filtering has been applied. The shape of the error distribution was not known.

To reduce the size of the inverse problem, unnecessary over-sampling of the airborne datasets is reduced by sub-sampling grids to a larger cell size, but one that was still below the Nyquist sampling rate given the low-pass filtering characteristics of these data. Also, the ground gravity grid previously continued to the output drape surface was re-sampled at the horizontal locations of the original observation to provide data as faithful to the original ground observations as possible.

Following analysis of the inversion results to verify a successful outcome, the response is predicted by forward modeling at regularly spaced locations on the output drape surface (Figure 2c). The first order trend surface removed from the data immediately prior to inversion is restored to produce the final grid of combined ground and airborne vertical gravity.

Application of the method

Example 1: West Arnhem Land Airborne Gravity Survey

Airborne gravity data were acquired with a GT-1A system over a survey area of 6875 km^2 in 2003 (Gabell and Tuckett, 2004). The airborne survey was commissioned after earlier attempts to acquire ground data had to be cancelled due to stalled land access negotiations (Duffett et al., 2004). Lines were flown east-west with 2 km spacing at a constant elevation of 655 m AHD. Tie-lines were flown north-south at 20 km spacing.

Ground measurements

Pre-existing ground gravity data in the vicinity of the survey area consisted of a grid of observations at roughly 11 km spacing and a number of more detailed traverses along roads and tracks (Fraser, Moss and Turpie, 1976). An essential ingredient of the combination method is the assignment of uncertainty to each gravity observation. Uncertainty in the ground vertical gravity Bouguer anomaly values was calculated using estimates of horizontal and vertical positioning accuracy and accuracy of the gravity observations themselves (Equations 1 to 3). Equation 1 is an approximation of the derivative of theoretical gravity with respect to latitude multiplied by the estimate of horizontal position error. Equation 2 is an approximation of the vertical derivative of the combined free-air and Bouguer corrections multiplied by the estimated vertical position error. Equation 3 combines the various error contributions assuming independence between the errors.

$$\varepsilon_{ht} \approx 0.01 \cdot h \cdot \sin 2\varphi \qquad \textit{Equation 1}$$

$$\varepsilon_{v} \approx -2 \cdot v \qquad \textit{Equation 2}$$

$$\varepsilon_{CBA} = \sqrt{\left(\varepsilon_{ht}^{\ 2} + \varepsilon_{v}^{\ 2} + \varepsilon_{obs}^{\ 2} + \varepsilon_{tc}^{\ 2}\right)} \qquad \textit{Equation 3}$$

ε_{ht} is the vertical gravity error in μm/s^2 associated with uncertainty in horizontal positioning, h is the uncertainty in horizontal position in metres, φ is the latitude in degrees north, ε_v is the error in μm/s^2 for simple Bouguer anomaly vertical gravity due to uncertainty in vertical positioning (based on a correction density of 2670 kg/m^3), v is the uncertainty in vertical position in metres, ε_{obs} is the vertical gravity observation error in μm/s^2, ε_{CBA} is the uncertainty in the accuracy of complete Bouguer anomaly values in μm/s^2, and ε_{tc} is the uncertainty in the accuracy of terrain corrections in μm/s^2. The combination with airborne gravity data was based on simple rather than complete Bouguer anomaly values, so the uncertainty in terrain corrections was assumed to be common to both datasets and set to zero. The estimated uncertainty values ranged from 2 μm/s^2 to 10 μm/s^2.

Airborne measurements

The GT-1A airborne gravity system is described by Gabell and Tuckett (2003, 2004). Although complete Bouguer gravity anomaly values were produced from the airborne data, terrain corrections were not available for the ground observations. The two datasets were thus integrated using simple Bouguer anomaly values. For the data used in this study, the most significant filtering was done with a 107 second Kalman filter. At an

average aircraft speed of 69.1 m/s, 107 seconds corresponds to 7.4 km. The filter response is plotted using symbols in Figure 3b, where it is shown that this filter can be approximated by a 7th order Butterworth filter with midpoint wavelength (i.e., the wavelength where the response is reduced by half) of 8.2 km. An average spectrum for the data calculated in the flight line direction (Figure 3a) shows the expected decline in signal amplitude with decreasing wavelength for wavelengths less than 10 km. The marked drop in amplitude for wavelengths shorter than 10 km is consistent with the impact of the Kalman filter shown in Figure 3b.

Results from a number of different investigations were used as inputs to obtain the final estimate of uncertainty in the airborne gravity data of 10 µm/s^2 for wavelengths between 8 and 55 km. Differences in data values where flight lines and tie lines intersect provide an indication of data uncertainty. The mistie values vary depending on the nature of the leveling that has been applied to the data. The standard deviation of the misties was 21.7 µm/s^2 for raw data, 10.3 µm/s^2 after leveling using low order trends, and 3.7 µm/s^2 after final leveling adjustments (Gabell and Tuckett, 2004). A 10 km portion of one of the flight lines was flown 5 times. The precision of the measurements for this repeat line was estimated as 5.2 µm/s^2 using the procedure described by Green and Lane (2003). Differences from one pass along the line to the next that arise from wavelengths longer than the length of the line are excluded from this precision estimate. Thus, the precision estimate is only valid for data that have been high-pass filtered to exclude wavelengths greater than the length of the repeat line (i.e., 10 km in this instance). The uncertainty would be larger if longer wavelength information were also considered. This was the case when the differences between upward continued ground gravity measurements along a 55 km traverse and the final airborne data were examined. The standard deviation of the differences was 10.6 µm/s^2. This was considered the best estimate of the uncertainty in the data, although even this figure must be qualified as referring to data where wavelengths in excess of 55 km have been removed.

Although the airborne data were tied to the Australian Fundamental Gravity Network (Gabell and Tuckett, 2003), there remained long wavelength discrepancies between the existing ground data, upward continued to the height of the airborne survey, and the airborne data. To reduce this discrepancy, a crossover filter was applied to the ground and airborne data. This involves high-pass filtering of the airborne data and replacing the low frequency portion of this dataset with low-pass filtered ground data. The crossover wavelength is chosen based on sample spacing and accuracy considerations.

The complementary high and low-pass filter response functions defined by a cosine roll-off between 35 and 45 km are illustrated in Figure 4. Given a basic sample spacing of 11 km for the ground data, significant aliasing for wavelengths less than 22 km would be expected for these data. The smallest dimension of the survey area, around 60 km, dictates that longest wavelength that will be properly sampled in the airborne data. The crossover wavelength bracket of 35 to 45 km was chosen as midway between these wavelength constraints. An image of the difference between the crossover filtered product and the original airborne data is shown in Figure 4. The image represents the differences for wavelengths greater than 40 km between the ground and airborne data. There is an average offset of around -20 µm/s^2, with indications of a trend from around zero offset in the northwest to around -40 µm/s^2 in the southeast. Having reduced the wavelength range of the AG contribution in the filtered output from 8-60 km to 8-40 km, the noise estimate was revised downward to 8 µm/s^2. This does not imply that the ground gravity data are noise-free for wavelengths greater than 40 km. When it comes to combining the ground data with the output of the crossover filter, these data are identical for wavelengths greater than 40 km, and hence no allowance for inconsistency is required for these wavelengths.

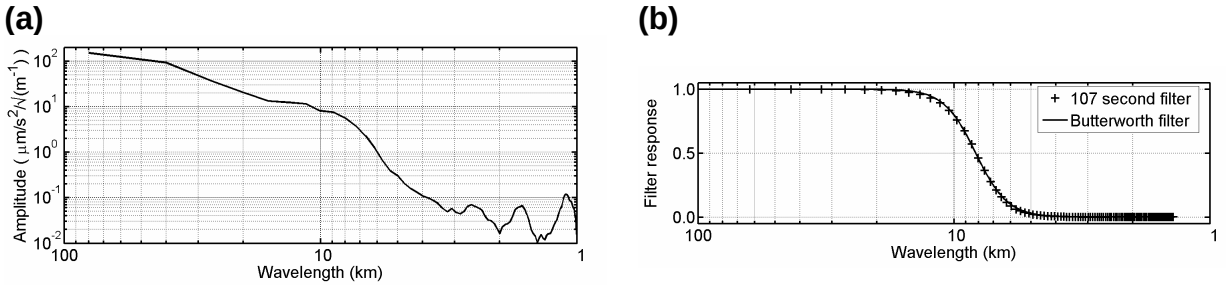

Figure 3. (a) Average amplitude spectrum of West Arnhem Land AG simple Bouguer anomaly data, calculated in the flight line direction (090 or 270 degrees). (b) Filter response for 107 second Kalman filter (symbols) as given by Gabell and Tuckett (2003) and filter response for 7th order Butterworth filter with central wavelength of 8.2 km (solid line).

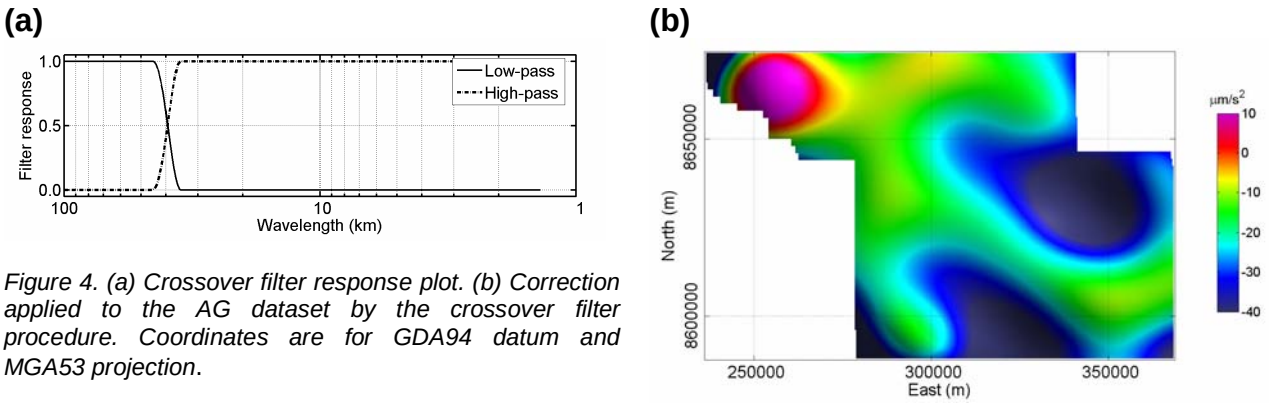

Figure 4. (a) Crossover filter response plot. (b) Correction applied to the AG dataset by the crossover filter procedure. Coordinates are for GDA94 datum and MGA53 projection.

Combined ground and airborne measurements

The airborne data were acquired at a constant height of 655 m AHD (i.e., constant height above the geoid). This flat surface was chosen as the output drape surface to eliminate the need to continue the airborne data to another surface. To reduce the computational load during equivalent layer inversion, the airborne data were up-sampled to 1600 m spacing from the original 400 m grid. This spacing is still well below the 4 km sampling required to capture wavelengths above the 8 km central value of the low-pass filter applied to the airborne data.

The ground data were gridded with 400 m cells then continued from ground level to the output drape surface using a Fourier drape-to-level procedure described by Cordell and Grouch (1985). The data used for the inversion were derived by re-sampling the continued grid at the horizontal locations of the original observations.

The performance of the equivalent source inversion was assessed by reviewing the overall data misfit, histograms of the normalized data misfit, mass properties of the equivalent source layer, the spatial distribution of data misfit values and the vertical gravity predictions on the output drape surface.

The expected value for the chi-squared noise-weighted (“normalized”) data misfit is equal to the number of observation points. This assumes that the data errors are approximately normally distributed, the model structure is not an impediment to obtaining a close fit to the data (i.e., that the model layer is not too far below the observations, that the model elements are not too coarse, etc) and the supplied error levels are sufficiently large that any inconsistencies between the ground and airborne data can be resolved without exceeding the expected value of the chi-squared noise-weighted data misfit. The inversion finds a solution that is consistent with the data errors in the sense that the regularization is adjusted to obtain a data misfit with the expected chi-squared value. After each inversion, histograms of normalized data misfit were inspected to see if the distribution of the normalized data misfits approximated a normal distribution. (Figure 5). The number of observations (“N”) and the chi-squared normalized data misfit (“chi_sq”) is printed in the top right of each of these histograms. Histograms were produced for the combined dataset and for the ground and airborne data separately. This provided a check that the relative errors between the ground and airborne data had been set appropriately. Although the normalized data misfit values did not perfectly match a normal distribution, the observed distributions were considered to be acceptable.

A smooth lateral variation in the mass properties of the equivalent layer was sought to ensure an appropriately smooth fit to the data, particularly in areas with sparse observations. The inversion algorithm automatically adjusts the trade-off parameter between the model objective function and the data misfit so that the desired degree of fit to the data is obtained. The model objective function has two components: lateral smoothness and smallness. The smoothness constraint is the sum of differences between adjacent cells in the east-west and north-south directions, whilst the “smallness” constraint is the sum over all cells of the differences between the density values and the reference density. The latter was everywhere zero in this instance. The variations in the mass properties of the layer can be strongly influenced by factors other than the data and the data errors: the dimensions of the cells, the separation between the top of the cells and the observations, and the relative weighting of smoothness and smallness constraints. In early inversion attempts, the lateral variation in mass properties was not sufficiently smooth (Figure 6). This was rectified by using model elements with smaller horizontal cross-section, greater depth extent and by increasing the smoothness weighting relative to the smallness weighting. Given the geometry of the equivalent layer, there is no direct connection between the mass properties within the layer and the actual subsurface density values in the survey area. The distribution of the properties does however represent a de-convolution of the vertical gravity response into a more focused form. This is evident in a comparison between Figure 6b and Figure 8c.

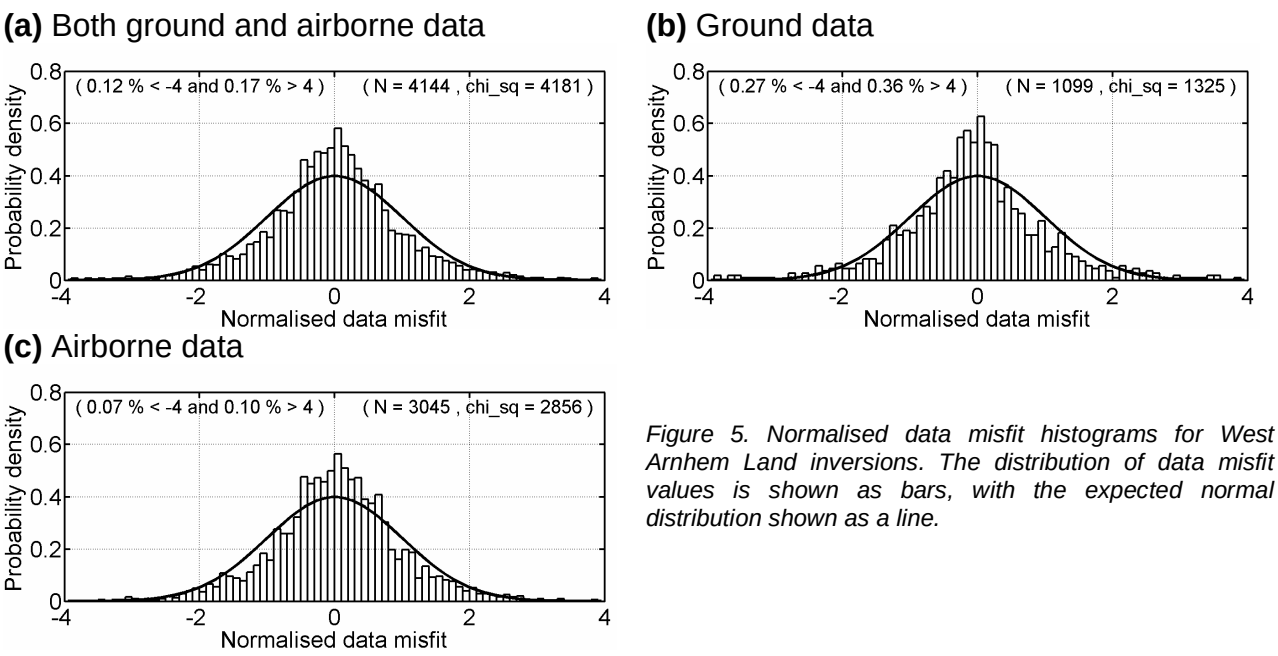

Figure 5. Normalised data misfit histograms for West Arnhem Land inversions. The distribution of data misfit values is shown as bars, with the expected normal distribution shown as a line.

The performance of each inversion was further analyzed by displaying grids of the data misfit for the input ground and airborne datasets (Figure 7). If the correct noise estimates and inversion parameters have been used, there should not be any signal present in these grids. This is more or less the case in the final inversion, though there is a hint of coherent geological structure near the western edge of the survey in the image of airborne data misfit.

Once a satisfactory inversion was obtained, the response was calculated by forward modeling of the equivalent layer mass properties at the desired output spacing of 400 m on the output drape surface (Figure 8). The first order trend surface removed from the data prior to inversion was then restored (not shown). This output represents an optimized combination of the ground and airborne simple Bouguer vertical gravity data.

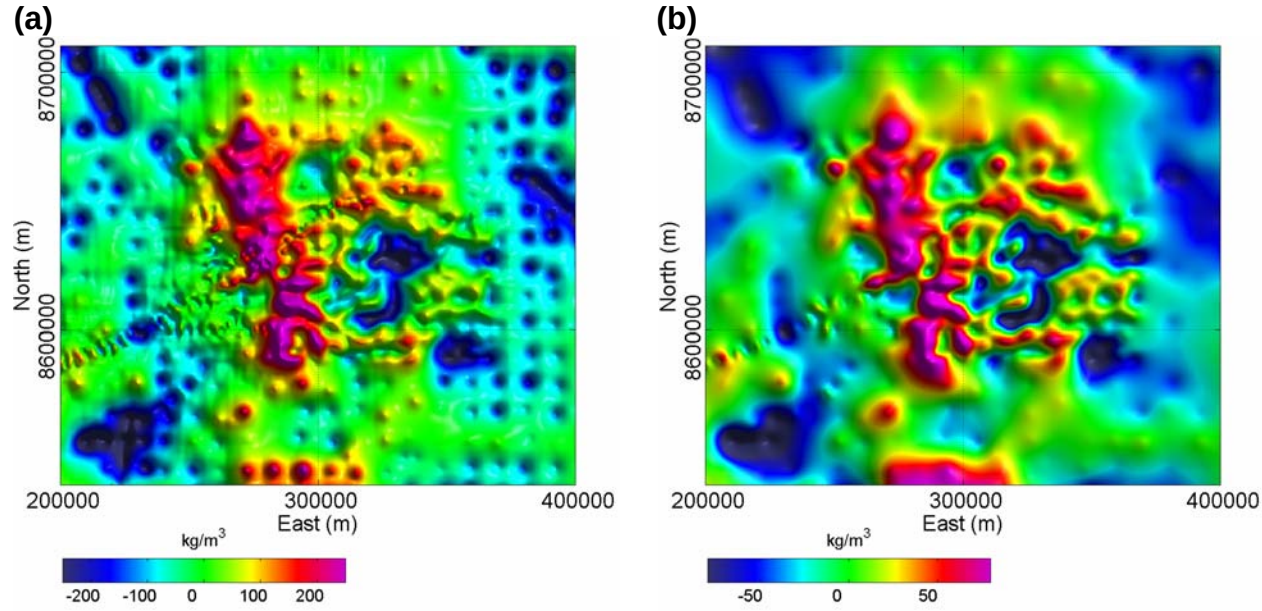

Figure 6. Images of equivalent layer density values. Both inversions fit the observations to the prescribed level of uncertainty. (a) Early inversion result showing inappropriate lateral smoothness in the mass properties of the layer. The model elements were 1600 m below the level of the observations, and had horizontal size 1600 m and vertical extent 2000 m. The weighting of smoothness to smallness model constraints was not high enough for smoothness to dominate. (b) Final inversion result. The model elements were 800 m below the level of the observations, and had horizontal size 800 m and vertical extent 8000 m. The smoothness model constraint was weighted so that it would dominate over the smallness model constraint.

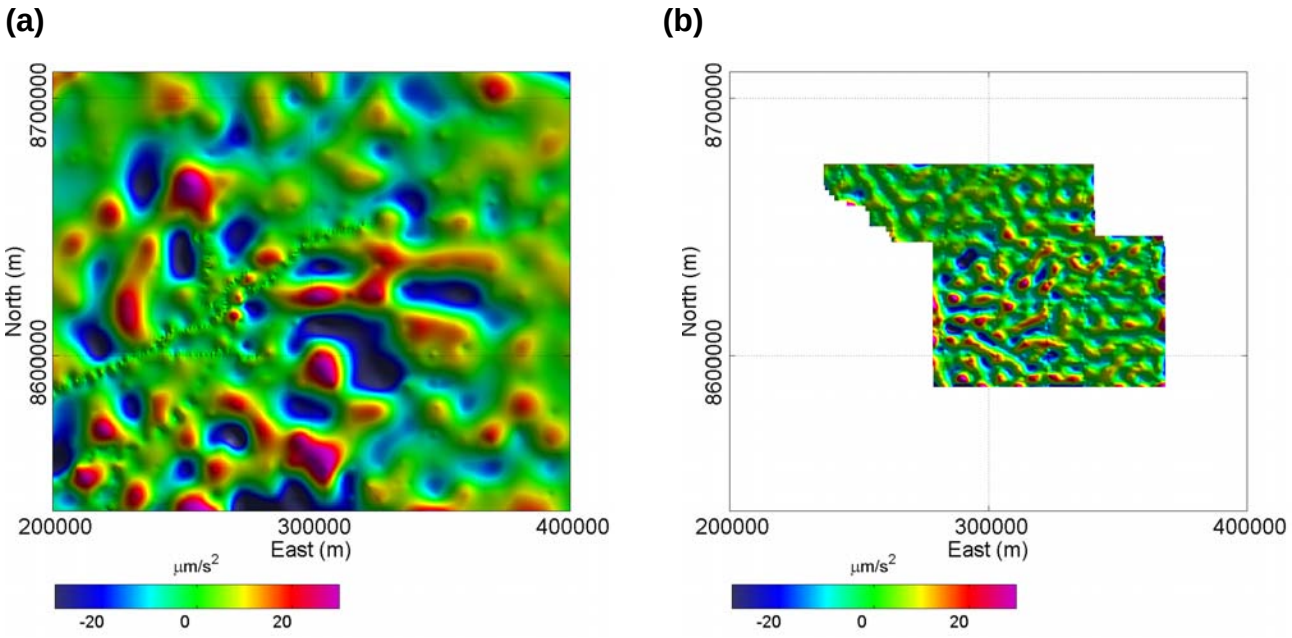

Figure 7. Data misfit images from the final inversion for (a) ground and (b) airborne data.

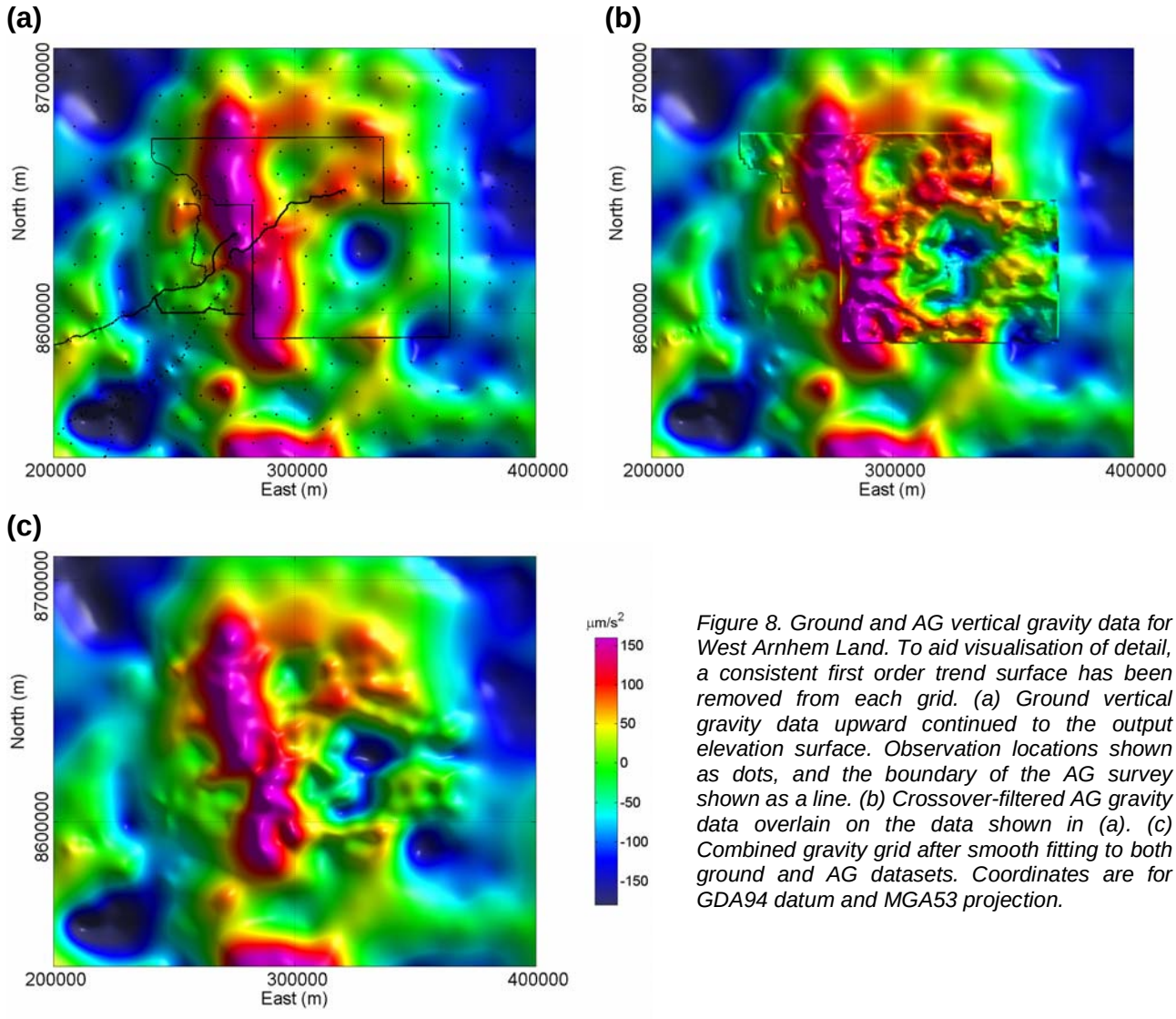

Figure 8. Ground and AG vertical gravity data for West Arnhem Land. To aid visualisation of detail, a consistent first order trend surface has been removed from each grid. (a) Ground vertical gravity data upward continued to the output elevation surface. Observation locations shown as dots, and the boundary of the AG survey shown as a line. (b) Crossover-filtered AG gravity data overlain on the data shown in (a). (c) Combined gravity grid after smooth fitting to both ground and AG datasets. Coordinates are for GDA94 datum and MGA53 projection.

Example 2: Broken Hill Airborne Gravity Gradiometer Survey

A FALCON airborne gravity gradiometer survey was flown in the Broken Hill district early in 2003 to stimulate exploration for base metal, Fe-Cu-Au and Ni-Cu-Pt-Pd deposits (Lane et al., 2003). The survey covered an area of 1186 km^2, with lines flown in 036 and 216 directions at 200 m spacing. The tie lines had 2000 m spacing and the nominal terrain clearance was 80 m (Fugro Airborne Surveys, 2003).

Ground measurements

The pre-existing ground gravity data were acquired over a very large number of acquisition campaigns, with different levels of accuracy and sample spacing. Within the survey area, the maximum sample spacing is 2 km. Some very detailed grids of observations are present, with data acquired at 25 to 50 m spacing on lines 100 to 200 m apart. Using information provided in acquisition and processing reports, estimates of uncertainty in the simple Bouguer gravity values were calculated as per the expressions in Equations 1 to 3. The uncertainty values ranged from 0.5 to 10 µm/s^2, with an RMS value around 1.5 µm/s^2.

Airborne measurements

The FALCON AGG system is described by Lee (2001). Given that two horizontal gradients are measured over the survey area, either or both of the gradients can be transformed to any other gravitational quantity, including vertical gravity. This transformation can be carried out using one of several methods and vertical gravity data were provided from the Broken Hill Survey based on equivalent source and Fourier. These results are not identical because of differences in the assumptions involved and differences in the numerical methods used to treat noise in the gradient data (Hensley, 2003a). In this study, the vertical gravity derived via the Fourier method was used. A low pass filter with a cutoff wavelength of 400 m had been applied to these data. Dransfield et al. (2001) indicate that a 6th order Butterworth filter is used for this filtering. An average amplitude spectrum calculated in the flight line direction from the Fourier method vertical gravity data is shown in Figure 9a. The filter response spectrum for a 6th order Butterworth low-pass filter with a central wavelength of 400 m is shown in Figure 9b for comparison. The rapid attenuation of amplitude for wavelengths less than 500-600 m that is observed in the Broken Hill data is consistent with the given filter response spectrum.

Liu et al. (2001) and Dransfield et al. (2001) indicate that system noise in Falcon AGG data is closely related to the level of turbulence experienced during acquisition. Short duration turbulence events would introduce broadband noise into the measurements. Given decreasing levels of signal with decreasing wavelength, such noise would become a limiting factor at short wavelengths. Accuracy at long wavelengths in vertical gravity data from the system is limited by processing factors. Strictly speaking, transformation of one gravity quantity to another requires knowledge of the response over an infinite extent. Given data from a finite survey area, the maximum wavelength that can be present in the transformed data is related to the dimensions of the survey area. Long wavelength accuracy is further affected because only relative gravity gradients are measured (Dransfield et al., 2001). This means that neither absolute level nor first order trend information in the vertical gravity field will be recovered.

A portion of a flight line was flown on 5 separate occasions in the course of the Broken Hill survey to provide data for an estimate of “repeatability” or precision (Hensley, 2003b). It was not appreciated at the time, however, that a repeat swath rather than a repeat line would be required to meet this objective. Given that spatial transformations are used to produce both gradient and vertical gravity data, the repeat line data were processed using a surrounding set of flight lines that were the same for processing of each separate pass. This violated the assumption required for deriving precision estimates from repeat line data that all of the data involved in processing one pass along the repeat line are independent from the data used for processing any other pass along the line. Consequently, the precision estimates derived from this exercise underestimate the variability in the vertical gravity data. Ground data with sufficient detail and accuracy to be used for estimating the noise level in the AGG data are of limited spatial extent, and hence of limited use for this purpose. Boggs and Dransfield (2003) provide an estimate of the noise in Falcon AGG vertical gravity data. They estimate the noise to have a spectral density of 1 µm/s^2/$\sqrt{}$(km). Thus, for the Broken Hill survey with wavelengths present up to 20 km, noise levels of around 0.4 µm/s^2 might be anticipated.

To reduce the inconsistency between the ground and airborne data at long wavelengths, a crossover filter procedure was applied. Long wavelength information in the airborne data was replaced with the relevant portion of the ground vertical gravity data spectrum following upward continuation of the ground data to the drape surface for the airborne observations. The maximum spacing between ground gravity observations was 2 km. Thus, wavelengths of 4 km and above are fully sampled. The minimum survey dimension is 20 km, so wavelengths of 10 km or less should be recovered with reasonable accuracy in the AGG data. Various crossover wavelength ranges between 4 and 10 km were trialed before settling on a range of 4-6 km (Figure 10). The image of differences between the airborne data and the crossover filter output shows an

average offset of around 110 µm/s^2 was present between the airborne and ground datasets. An offset of this magnitude was not surprising since the relative gradient measurements do not allow the absolute level of vertical gravity to be recovered. Figure 10b shows that other long wavelength differences of up to 40 µm/s^2 are also present. Based on values extracted at the horizontal position of the original ground observation locations, the standard deviation of the differences between ground data and the airborne data following crossover filtering was 2.1 µm/s^2. This figure is consistent with noise levels that would be predicted for airborne data with wavelength range limited to less than 5 km using the noise spectral density value derived by Boggs and Dransfield (2003) (i.e., 1 µm/s^2/√(km) over a bandwidth of 5 km is approximately 2.2 µm/s^2).

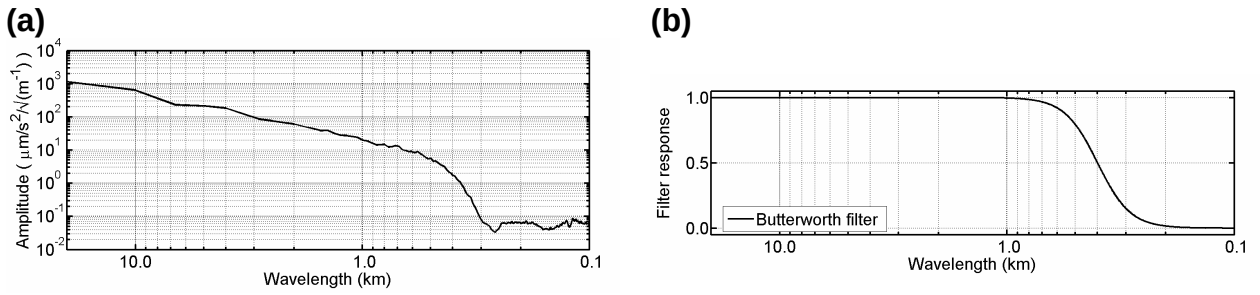

Figure 9. (a) Average amplitude spectrum of Broken Hill AGG vertical gravity data (Fourier method), calculated in the flight line direction (036 or 216 degrees). (b) Filter response for 6th order Butterworth filter with central wavelength of 0.4 km.

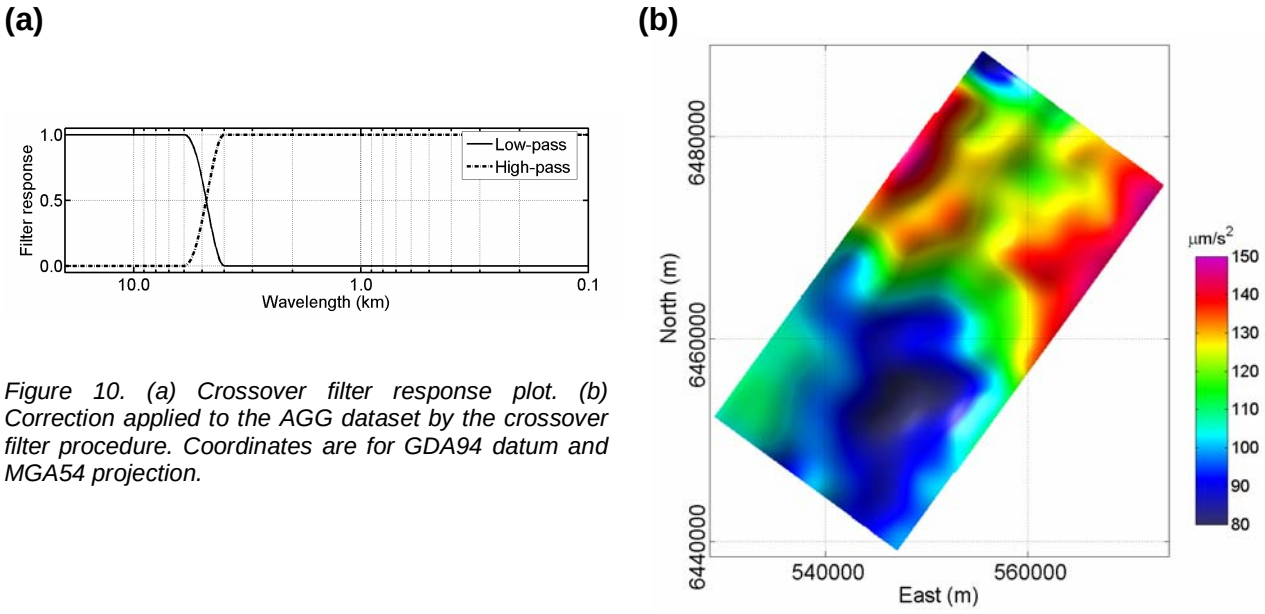

Figure 10. (a) Crossover filter response plot. (b) Correction applied to the AGG dataset by the crossover filter procedure. Coordinates are for GDA94 datum and MGA54 projection.

Combined ground and airborne measurements

The drape surface specified for the Fourier method AGG vertical gravity data was a smoothed version of surface topography offset upwards by 80 m. To avoid having to continue the airborne data, the output drape surface was chosen to coincide with this surface. The ground data were gridded, upward continued to the output drape surface then re-sampled at the horizontal location of the original observations. A first order trend surface was removed from both ground and airborne data prior to equivalent layer inversion so that the average mass property value required to reproduce the residual anomalies would be approximately zero.

Given the use of a 400 m low pass filter, the supplied grids of AGG data with 50 m cell size substantially over-sample the available information. To reduce the computational demands, the crossover-filtered airborne data were up-sampled to the maximum 200 m spacing. This spacing was matched to the horizontal dimensions of the cells in the equivalent source layer and the 200 m vertical separation between the observations and the equivalent source layer. Although it would have been preferable to retain a degree of over-sampling (e.g.,100 m cells, 100 m vertical separation between the observations and the top of the equivalent source layer, and 100 m samples of the airborne data), a substantially more efficient equivalent source inversion algorithm would have been required.

Images of the ground, airborne and combined data are shown in Figure 11. Owing to the large number and close spacing of the observations in this example, results of a vertical derivative applied to each of these grids are also given (Figure 12). These images of the vertical gravity gradient clearly illustrate the relatively seamless integration of ground and airborne data through the method outlined in this paper, as well as the resultant loss of short wavelength resolution that necessarily accompanies the procedure.

Figure 11. Ground and AGG vertical gravity data for Broken Hill. (a) Ground vertical gravity data upward continued to the output elevation surface. Observation locations shown as dots. (b) Crossover-filtered AGG gravity data (Fourier method) overlain on the data shown in (a). (c) Combined gravity grid after smooth fitting to both ground and AGG datasets. Coordinates are for GDA94 datum and MGA54 projection.

Figure 11(a) Ground vertical gravity data upward continued to the output elevation surface. Observation locations shown as dots.

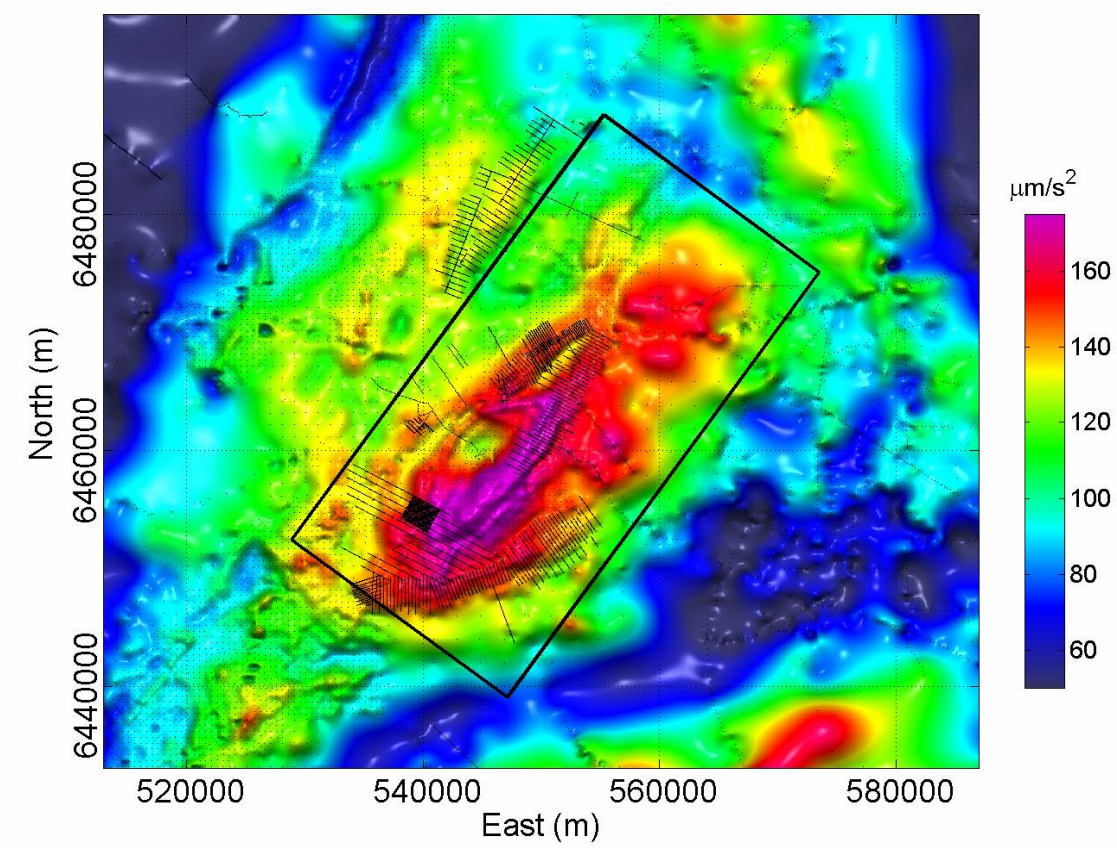

Figure 11(b) Crossover-filtered AGG gravity data (Fourier method) overlain on the data shown in (a).

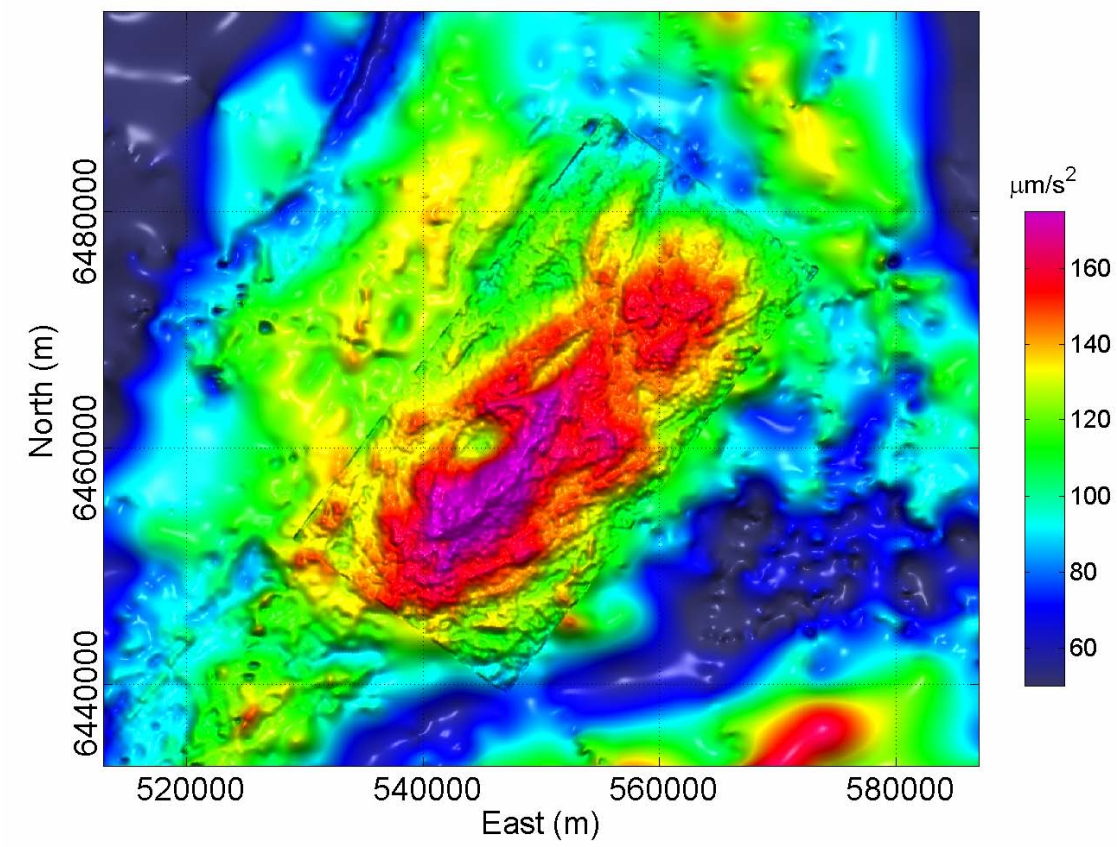

Figure 11(c) Combined gravity grid after smooth fitting to both ground and AGG datasets. Coordinates are for GDA94 datum and MGA54 projection.

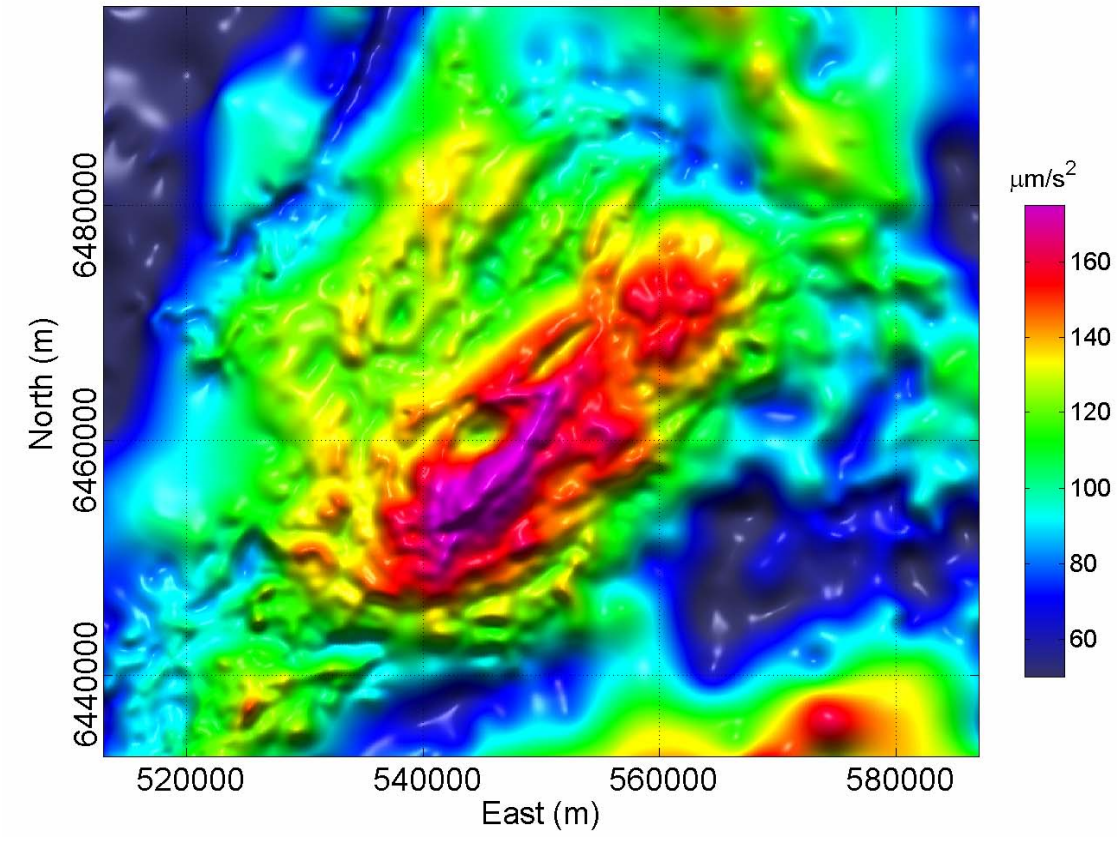

It is standard practice to use an exact fitting procedure such as minimum curvature gridding to grid potential field data. Short wavelength artifacts will be produced when noise-contaminated observations with variable spacing are present (Figure 11a). These short wavelength artifacts are given additional emphasis when a vertical derivative is applied to the grid of vertical gravity to produce a grid of the vertical gravity gradient (Figure 12a). The reduction in impact of these artifacts in the smooth-fitting grid (Figure 11c and Figure 12c) provides some justification for producing such a grid to complement the exact-fit grid. Although the benefit of a smooth-fitting procedure is a reduction in the level of short wavelength artifacts, the downside is a blurring of signal.

Figure 12. Ground and AGG vertical gravity gradient data for Broken Hill. (a) Ground vertical gravity gradient data upward continued to the output elevation surface. (b) Crossover-filtered AGG vertical gravity gradient data (Fourier method) overlain on the data shown in (a). (c) Combined vertical gravity gradient grid after smooth fitting to both ground and AGG datasets.

Figure 12(a) Ground vertical gravity gradient data upward continued to the output elevation surface.

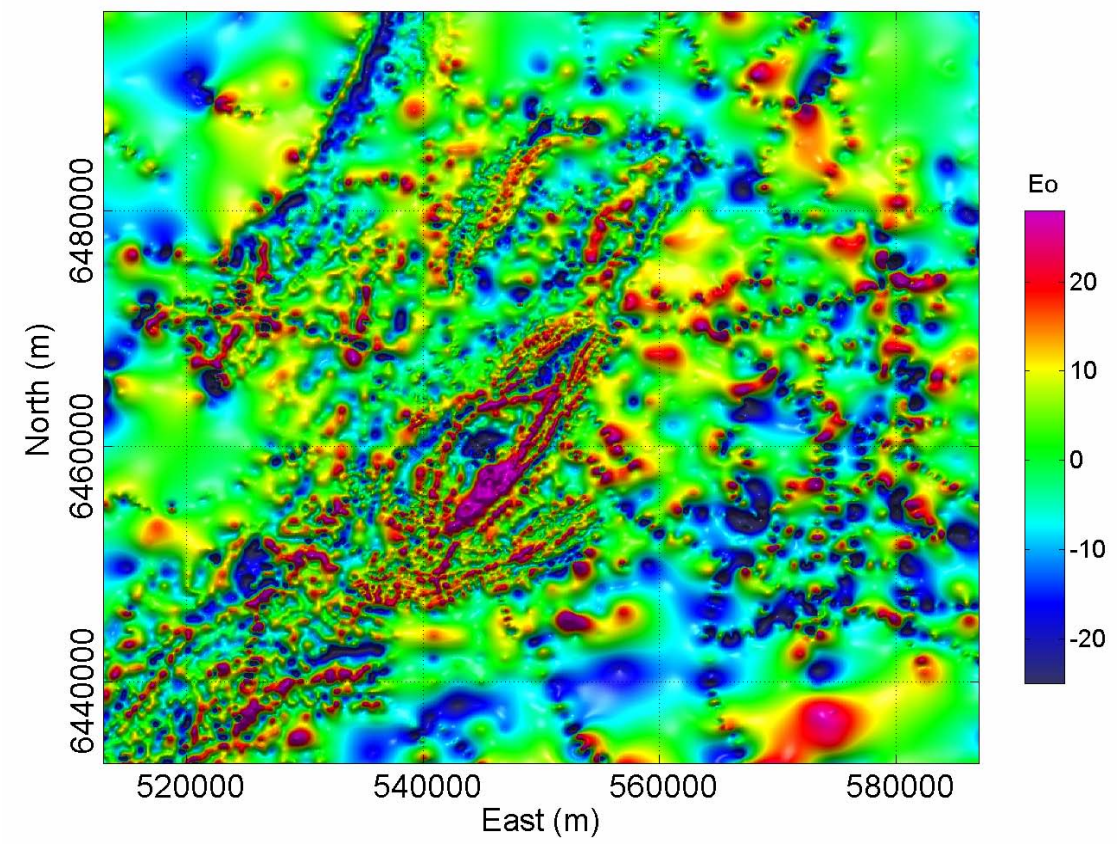

Figure 12(b) Crossover-filtered AGG vertical gravity gradient data (Fourier method) overlain on the data shown in (a).

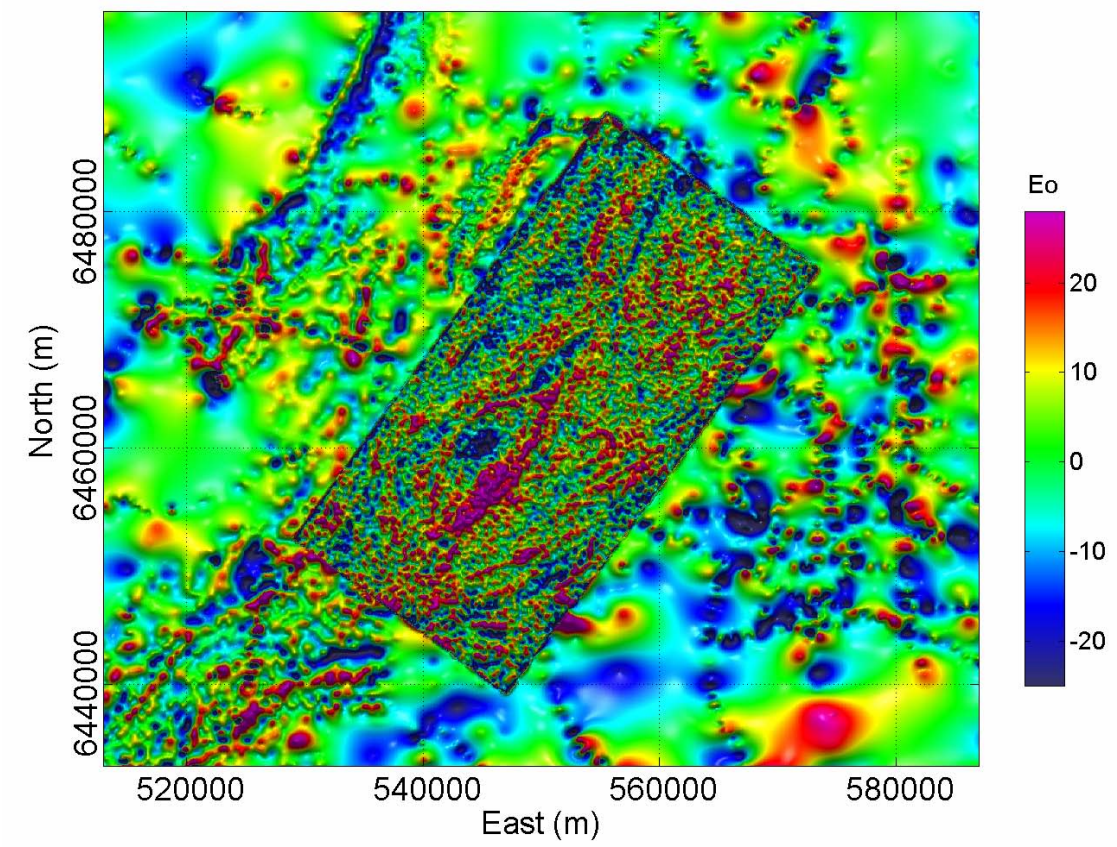

Figure 12(c) Combined vertical gravity gradient grid after smooth fitting to both ground and AGG datasets.

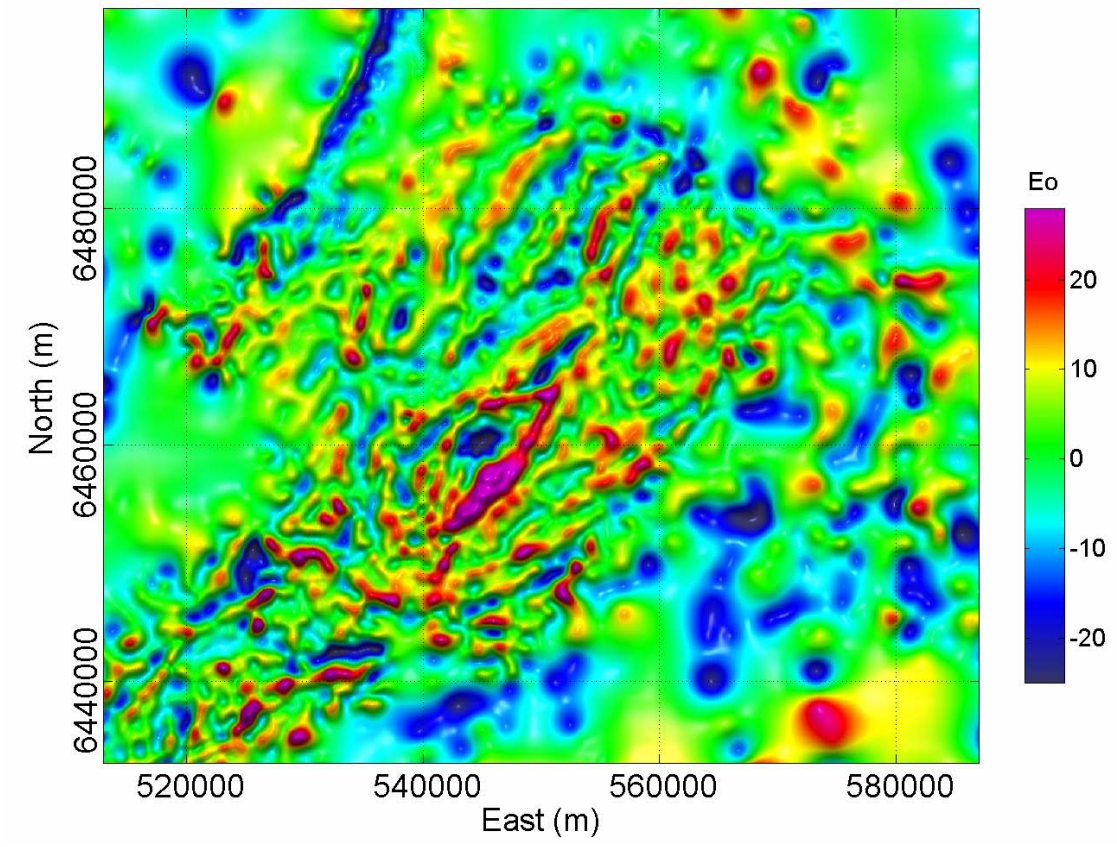

Discussion

The range of wavelengths present in each of the datasets examined is summarised in Figure 13. Limitations in the signals at either short or long wavelengths (or both) were observed in each of them. Ideally, the datasets used to produce a compilation would span the entire wavelength range with sufficient overlap to allow inconsistencies between the datasets to be resolved. It is more important to have adequate signal at mid to long wavelengths since most of the power in the vertical gravity signal is present in these wavelengths. Fortunately, the existing ground gravity coverage provides this for all onshore locations in Australia. There are deficiencies in the signal at short wavelengths in each of the datasets used in the examples, and hence in the combined products, but this does not preclude coherent regional appreciation of the mid to long wavelengths that are available.

The size of an airborne survey places restrictions on the wavelengths that can be recovered using either of the systems discussed in this study. Drift in the system response and the need to level the data plays a part in the processing of the AG data. Integration of a gradient response over a finite survey area is a restriction in the case of the AGG system. The deficiencies are not restricted to the absolute level or to the longest wavelength, but impact a number of the longer wavelength terms that are obtained by 2D Fourier decomposition. Longer wavelengths in the airborne data were replaced with more accurate and complete information from the existing ground gravity data. In both examples, there was sufficient overlap in wavelengths to allow this to be done. For an overlap to exist, the maximum spacing of the ground gravity observations within the airborne survey area must be less than half of the smallest dimension of the survey area. The maximum spacing of the ground gravity observations would preferably be less than a quarter of the smallest dimension of the survey area to allow for diminished accuracy at the shorter wavelengths in the ground data and the longer wavelengths in the airborne data. The maximum ground gravity station spacing anywhere in Australia is 11 km, so this condition will be met for surveys that are at least 22 km in size, and preferably at least 44 km in size across the smallest dimension.

Turbulence is noted as a major source of noise for both AG and AGG methods. At the time scales relevant to the resolution of the systems, turbulence would give rise to a random series of impulsive noise events with constant amplitude over all wavelengths. Given that the vertical gravity signal diminishes in amplitude with decreasing wavelength, the signal to noise will thus be smaller at short wavelengths. Low-pass filtering had been applied to both the AG and AGG datasets to restrict the visual impact of noise at short wavelengths, and the cut-off wavelength of this filter defined the short wavelength resolution of the data.

The wavelength chart in Figure 13 shows that acquisition of AG data in the Broken Hill area would not have produced new information. The existing ground data already provide information over the 8 to 80 km wavelength range of the AG data. Acquisition of AGG data in the West Arnhem Land area would also have been problematic, since this would have left only partial coverage of wavelengths between 10 and 44 km. It can thus be seen that consideration of the wavelength range that can be obtained from AG and AGG systems provides one criterion for deciding on the suitability of these methods for improving the gravity coverage in a given region.

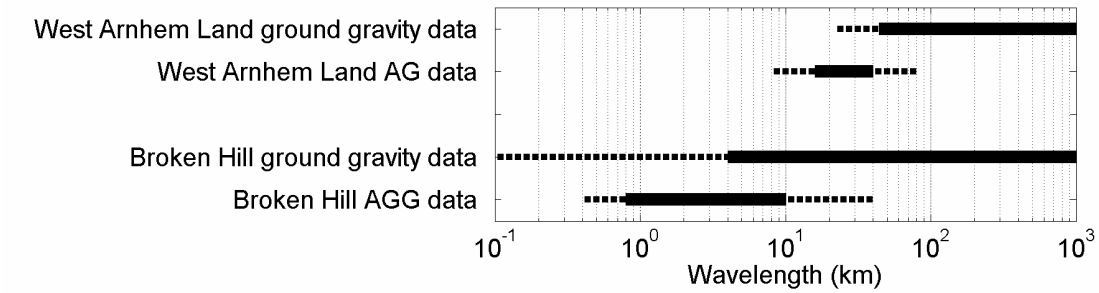

Figure 13. Chart of data source and estimated wavelength range. Solid lines indicate accurate data whilst dashed lines indicate either partial spatial coverage or reduced accuracy.

An equivalent source method was used to produce a smooth fit to the two input datasets. As noted by Billings et al. (2002a,b), this is one of a group of methods which can be described as radial basis functions. Other methods from this group, such as splines, kriging or collocation, could have been used in the fitting procedure. The equivalent source method was chosen in this instance because it directly models the gravity signal being considered. Although not unique amongst smoothing functions, the specific implementation of the equivalent source method used in this study had the desirable characteristic of producing a smooth fit that was adaptive to the spatial distribution of observations and to their individual noise estimates.

Conclusions

A multi-stage procedure for combining ground and airborne vertical gravity data was described and successfully applied to field examples involving data sourced from AG and AGG surveys. Although acquisition methods, output bandwidth and noise levels were very different for the two airborne datasets, the same procedure was found to be suitable when combining data from either of these systems with ground gravity data.

Since the ground and airborne data are associated with different elevation drape surfaces, there must be a conscious selection of an output drape surface. A drape-to-drape method was used to continue both datasets onto this surface.

Deficiencies were recognized in the long wavelength accuracy of both of the airborne datasets, brought about by the finite size of the survey areas and instrument drift. A crossover filtering method was used to replace the longer wavelengths in the airborne datasets with information from ground data.

The presence of noise means that there are inconsistencies between the data values where the datasets overlap, and hence it is not possible to exactly fit a surface to both datasets. An equivalent source method was used to construct a density model that produced a smooth vertical gravity response that approximately fitted both datasets. Smoothness constraints on the lateral variability in the mass properties of the sources allowed a smooth rather than exact surface to be fit to the data. The misfit between the input and fitted data was dependent on the noise levels assigned to each individual observation. A regular grid of output data values was generated by forward modeling the equivalent source distribution at specified locations on the output drape surface.

It was noted that a smooth-fitting method can complement the usual exact-fitting method used for gridding ground gravity data, regardless of whether these data are gridded alone or combined with airborne data. The uncertainty in ground data is sufficient to produce large artifacts at short wavelengths in grids produced using exact-fitting methods. These artifacts are suppressed in the smooth fitting grids. This benefit must be balanced against the attenuation of short wavelength signal.

A number of separate stages in the procedure could be eliminated and larger datasets could be combined if a more efficient equivalent source fitting program specifically designed for this task was available.

Acknowledgments

The West Arnhem Land Airborne Gravity Survey was a joint project between the Northern Territory Geological Survey (NTGS), Geoscience Australia, Cameco Australia Pty Ltd and Rio Tinto Exploration Pty Ltd. The Broken Hill Airborne Gravity Gradiometry Survey was a joint project between the NSW Department of Mineral Resources, pmd*CRC, Geoscience Australia, Gravity Capital and BHP Billiton. Thoughtful comments on drafts of this paper from Peter Milligan and Ian Hone were greatly appreciated. This paper is published with the permission of the Chief Executive Officer, Geoscience Australia.

References

Billings, S.D., Beatson R.K., and Newsam, G.N., 2002a, Interpolation of geophysical data using continuous global surfaces: Geophysics, 67, 1810-1822.

Billings, S.D., Newsam, G.N., and Beatson R.K., 2002b, Smooth fitting of geophysical data using continuous global surfaces: Geophysics, 67, 1823-1834.

Boggs, D.B., and Dransfield, M.H., 2003, Analysis of errors in gravity derived from the FALCON Airborne Gravity Gradiometer: Submitted for inclusion in M. Talwani and E. Biegert (eds), Gravity Gradiometry – Instrumentation, Processing and Case Studies, Society of Exploration Geophysicists. (Reproduced as a paper in this volume).

Bruton, A.M., 2000, Improving the Accuracy and Resolution of SINS/DGPS Airborne Gravimetry: Ph.D Thesis, The Department of Geomatics Engineering, University of Calgary, UCGE Report No. 20145. (http://www.geomatics.ucalgary.ca/Papers/Thesis/KPS/00.20145.AMBruton.pdf)

Cordell, L, and Grauch, V.J.S., 1985, Mapping basement magnetization zones from aeromagnetic data in the San Juan Basin, New Mexico: in Hinze, W.J., (ed.), The Utility of Regional Gravity and Magnetic Anomaly Maps, Tulsa, Society of Exploration Geophysicists, 181-197.

Dransfield, M., Christensen, A., Rose, M., Stone, P., and Diorio, P., 2001, FALCON test results from the Bathurst Mining camp: Exploration Geophysics, 32, 243-246.

Duffett, M., Bacchin, M., and Lane R., 2004, West Arnhem Land Airborne Gravity Survey: In Record of Abstracts, Annual Geoscience Exploration Seminar (AGES) 2004, Northern Territory Geological Survey Record 2004-001.

Fraser, A.R., Moss, F.J., and Turpie, A, 1976, Reconnaissance gravity survey of Australia: Geophysics, 41, 1337-1345.

Fugro Airborne Surveys, 2003, Acquisition and Processing Report, Job 1572, Broken Hill, NSW, Airborne Gravity Gradiometer and Magnetic Geophysical Survey for BHPBilliton.

Gabell, A.R., and Tuckett, H., 2003, Final Report for GT1-A Demonstration Project: Zuisin Technology and Canadian Micro Gravity Pty Ltd.

Gabell, A.R., and Tuckett, H., 2004, Acquisition and processing report for Project 200380 West Arnhem Land, Northern Territory, GT-1A Airborne Gravity Survey: Fugro Airborne Surveys Pty Ltd (FAS Job No. 1608) and Canadian Micro Gravity Pty Ltd (CMG Job No. 2003-2).

Green, A., and Lane, R., 2003, Estimating Noise Levels in AEM Data: Extended Abstract, ASEG 16th Geophysical Conference and Exhibition, February 2003, Adelaide.

Hensley, C., 2003a, Data Processing Report, Airborne Gravity Gradiometer Survey, Broken Hill, NSW, Australia: BHPBilliton Falcon Operations Report CR 10657 for Survey USN 142911122002.

Hensley, C., 2003b, Repeat Line Data for the Broken Hill FALCON™ Survey: BHPBilliton Falcon Operations Memorandum CM10047.

Hensley, C., 2003c, Merging of Ground Gravity and Falcon™ Airborne Gravity Gradiometry to constrain long wavelengths at Broken Hill: BHPBilliton Falcon Operations Memorandum CM10052.

Lane, R., Milligan, P., and Robson, D., 2003, An airborne gravity gradiometer survey of Broken Hill: In Peljo M., (compiler), 2003, Broken Hill Exploration Initiative: Abstracts from the July 2003 Conference: Geoscience Australia Record 2003/13, 89-92.

Lee, J.B., 2001, FALCON gravity gradiometer technology: Exploration Geophysics, 32, 247-250.

Li, Y., and Oldenburg, D.W., 1998, 3-D inversion of gravity data: Geophysics, 63, 109-119.

Liu, G., Diorio, P., Stone, P., Lockhart, G., Christensen, A., Fitton N., and Dransfield, M., 2001, Detecting kimberlite pipes at Ekati with airborne gravity gradiometry: Extended Abstract, ASEG 15th Geophysical Conference and Exhibition, Brisbane, August 2001.